Inelastic scattering of electrons from ionic crystals with a highly conducting overlayer

L. H. Dubois and G. P. Schwartz
AT&T Bell Laboratories, 600 Mountain Avenue, Murray Hill, New Jersey 07974

R. E. Camley
Department of Physics, University of Colorado, Colorado Springs, Colorado 80907

D. L. Mills
Department of Physics, University of California, Irvine, California 92717
(Received 31 August 1983)

The purpose of the present study has been to examine the manner in which inelastic electron scattering from ionic crystal surfaces is modified by the presence of a conducting overlayer as its thickness passes from the limit of zero coverage through two-dimensional film formation and then onto bulk growth. Specifically, we present both experiments and theory on the effects of thin (<17 Å) silver overlayers on the vibrational spectrum of gallium arsenide single-crystal surfaces. Clean (100) Te-doped GaAs samples are characterized by an intense surface optical phonon at 36.2 ± 0.5 meV and a weaker plasmon-phonon coupled mode at 12—13 meV, depending on the doping level. Both modes are completely screened by a (3.0 ± 0.3)-Å-thick uniform overlayer of silver in good agreement with theoretical predictions (assuming a silver overlayer with bulk dielectric properties). In addition, modes characteristic of the coupled Ag-GaAs system are observed. The effects of silver film thickness and metal island formation are also discussed.

I. INTRODUCTION

The inelastic scattering of low-energy electrons from ionic crystal surfaces has been examined in detail in the last decade both theoretically and experimentally.[1] The primary scattering process results from the interaction of the Coulomb field of the incoming electron with the electrostatic potential set up in the vacuum by oscillating surface and near surface atoms. The observed strong, small angle scattering is well described within the dipole approximation because the electron scatters from these electrostatic potential fluctuations when it is 50—100 Å above the crystal surface.

The purpose of the present study has been to examine the manner in which inelastic electron scattering is modified by the presence of a conducting overlayer as its thickness passes from the limit of zero coverage through two-dimensional film formation and then onto bulk growth. The primary emphasis has been the study of uniform metal overlayers, but experiments have also been performed on island films, yielding valuable information concerning the differences between two-dimensional and nucleated island growth. The use of electron-energy-loss spectroscopy (EELS) to distinguish between these two growth mechanisms at very low coverages constitutes a rather unique and complementary technique to established methods such as low-energy electron diffraction (LEED) and reflection high-energy electron diffraction (RHEED).

The system chosen for our studies was Ag/(100) GaAs under conditions where the substrate temperature was held at ~ 170 K during metal deposition. This particular choice was dictated by two major considerations: (1) the use of a metal which does not display strong overlayer-substrate reactions and (2) the necessity to have a material which develops metalliclike properties at low coverages in order to be able to model the metal dielectric properties by their bulk values. Previous studies of Ag/(100) GaAs indicate that both of these considerations are reasonably well met by this system.[2,3]

The paper will be organized as follows. In Sec. II, we present experimental details relevant to the high-resolution EELS spectrometer, the measurement of Auger and LEED data, and the details of metal deposition. Section III contains the experimental results and outlines the trends which must be explained, and Sec. IV provides the theoretical background and discussion necessary to understand the manner in which the overlayer structure modifies the inelastic electron scattering. Section V summarizes our findings for both uniform overlayers and metallic islands.

II. EXPERIMENTAL

Experiments were carried out in an ultrahigh vacuum chamber operated in the range $5-8\times10^{-11}$ Torr except during metal deposition. The electron-energy-loss spectrometer design is similar to that described by Sexton[4] with the following instrument parameters. The incident electron beam contacts the sample at 60° relative to the surface normal at an impact energy of ~ 5 eV. Beam currents were typically $1-2\times10^{-10}$ A. Electrons were collected within $\sim\pm1°$ of the specular direction. The elastic scattering peak intensity from clean GaAs was of order 5×10^4 counts/sec; silver deposition reduced this intensity

by roughly two orders of magnitude. All EELS measurements were performed at ~ 170 K.

Derivative Auger spectra were collected with 1-kV excitation for transitions below 550 eV and with 3-kV excitation for the high-energy Ga and As transitions. The peak-to-peak modulation voltage was 1 V in all cases and beam currents of 5—10 μA were used. LEED patterns were examined at energies below 150 eV with beam currents in the μA range. As a general precaution to avoid electron beam artifacts, energy-loss spectra were always recorded prior to exposing the sample to either Auger or LEED analysis.

Bromine-methanol polished (100) GaAs wafers Te-doped to $n \sim 1\times 10^{17}$ cm^{-3} were etched in 1:1 HF:H_2O and mounted in the vacuum chamber. Clean surfaces were prepared by argon ion etching at 500 eV for 30—40 min (5×10^{-5} Torr) followed by annealing at 725 K for ~ 2 h. After cooling, the samples displayed a sharp (4×1)-45° LEED pattern and common contaminants such as C, O, and S were not detected by the Auger analysis.

Silver was evaporated from a liquid-nitrogen shrouded effusive oven and the flux measured with a quartz crystal oscillator calibrated against a Dek-Tac. The source-to-sample distance was ~ 25 cm, thus ensuring a uniform silver coverage over at least a 1-cm^2 area. The metal-deposition rate used throughout this study was 1.7 ± 0.2 Å/min. The sample was held at ~ 170 K during silver deposition and during all EELS-Auger-LEED measurements unless otherwise stated. The chamber pressure remained below 4×10^{-10} Torr during metal evaporation. Auger analysis, performed several hours after each metal deposition, showed contamination levels of less than a few percent of a monolayer in all cases.

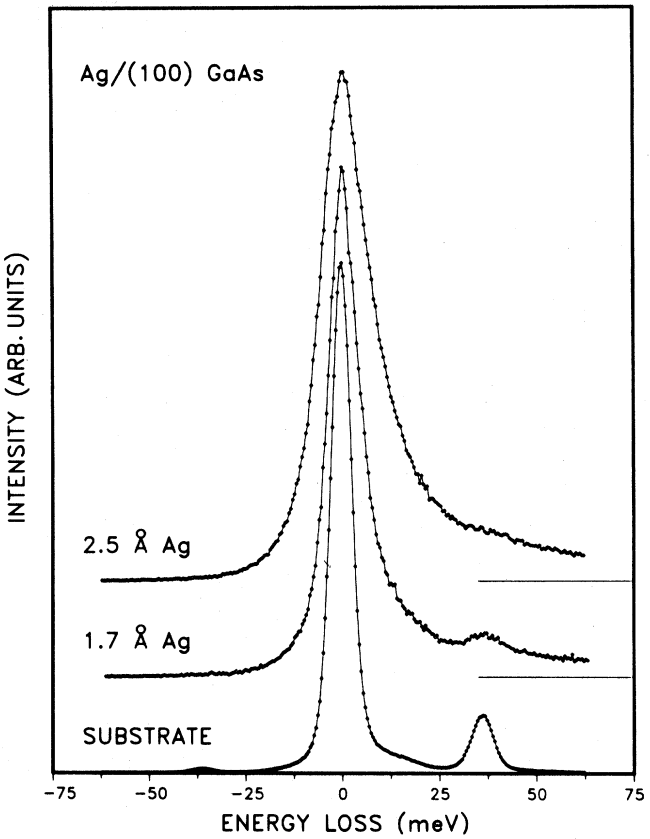

FIG. 1. The lower curve is a high-resolution EELS spectrum of a clean Te-doped ($\sim 1\times 10^{17}$ cm^{-3}) (100) GaAs surface taken at 170 K. The assignment of the peaks is discussed in the text. The middle trace shows the same surface after the deposition of an ~ 1.7-Å-thick uniform layer of silver at 170 K. The upper curve is the EELS spectrum of a 2.5-Å-thick layer also deposited with the substrate at 170 K. Baselines for each spectrum are shown to the right.

III. RESULTS

A. Uniform silver films

The lower trace of Fig. 1 shows the energy-loss spectrum associated with bare (100) GaAs in the absence of any Ag overlayer. The data points are spaced ~ 0.5 meV apart and are only connected for clarity of presentation. The curves have not been smoothed. The baseline for each spectrum is shown by the horizontal solid line to the right. Energy-loss (Stokes) peaks are shown plotted with positive energy relative to the elastic peak whereas energy-gain (anti-Stokes) peaks are assigned negative energies. The latter are symmetrically displaced relative to the elastic peak but their intensity is reduced by $n(\omega)/(n(\omega)+1)$, where $n(\omega)$ is the Bose-Einstein thermal factor. Since our measurement temperature (~ 170 K) strongly suppresses the anti-Stokes intensity, we will emphasize only the Stokes component in describing our results.

For GaAs doped in the range $n \sim 1\times 10^{17}$ cm^{-3}, there are two primary sources which contribute to the observed structure seen at 36.2 ± 0.5 and at ~ 12—13 meV. The first source is coupling of the substrate plasmon oscillations with the surface optical phonon. This contributes two modes denoted by $\tilde{\omega}_{\pm}$. The frequency and intensity dependence of these modes on the near-surface free-carrier concentration has been considered in detail elsewhere.[5,6] At this doping level the $\tilde{\omega}_+$ mode lies close to the unscreened surface optical phonon frequency of 36.2 meV, whereas the $\tilde{\omega}_-$ mode is seen at 12—13 meV. The second source of structure in the GaAs clean surface EELS spectrum is due to band bending. This band bending (~ 0.8 eV) creates a space-charge layer of approximate width 870 Å and, within the depletion approximation, this region contains no free carriers. As a consequence, scattering from the unscreened surface optical phonon will be detected at ~ 36.2 meV superimposed on the $\tilde{\omega}_+$ mode.

High-resolution EELS spectra associated with the buildup of an Ag overlayer are shown in Figs. 1 and 2 for deposited metal thicknesses of 1.7, 2.5, 3.4, and 17 Å. The justification for assigning these spectra to uniform silver overlayers will be presented in the next section. For a 1.7-Å silver film (middle curve of Fig. 1), the elastic peak is clearly broader than that of the clean surface (9.5 vs 6.5 meV) and is approximately 100 times less intense. More importantly, the surface optical phonon intensity has decreased significantly and a large, uniform background extending beyond 65 meV is observed. The deposition of a 2.5-Å-thick silver film further broadens the elastic peak width to 16.0 meV (Fig. 1, upper curve). The surface opti-

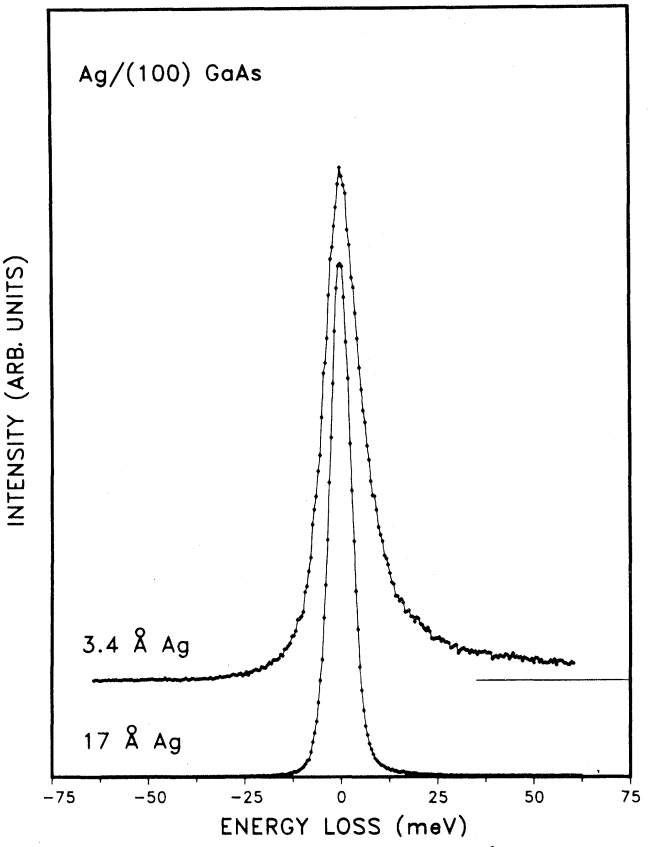

FIG. 2. High-resolution EELS spectra of 3.4-Å (upper curve) and 17-Å (lower curve) overlayers of Ag/(100) GaAs at 170 K.

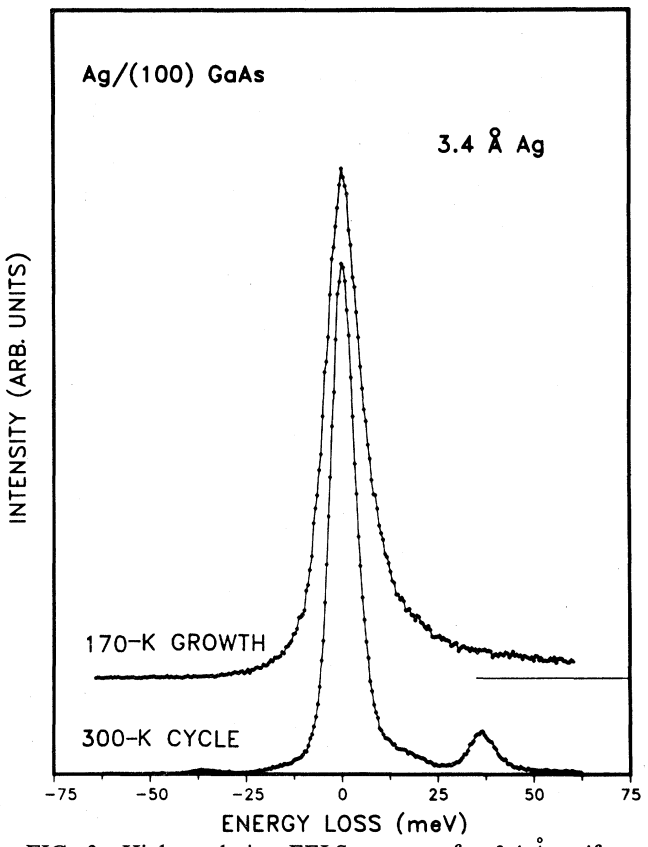

FIG. 3. High-resolution EELS spectra of a 3.4-Å uniform silver overlayer grown at 170 K (upper trace) and after slowly warming to room temperature overnight (lower trace).

cal phonon has now almost disappeared into the increasing background intensity. With a 3.4-Å-thick overlayer of silver deposited onto the GaAs substrate, the surface optical phonon peak is no longer detected (upper curve of Fig. 2). By this coverage the thin metal overlayer has completely screened the electric field of the oscillating substrate atoms. Furthermore, the elastic peak has begun to narrow [11.3 meV full width at half maximum (FWHM)] and the background intensity has dropped. Finally, with the growth of a ~17-Å-thick silver overlayer (Fig. 2, lower curve) only scattering from a thin metal film is observed; the elastic peak is approximately one order of magnitude more intense, narrower (6.5 meV FWHM), symmetric, and the background intensity is low.

The EELS observations which must be reconciled with theory can be summarized as follows. (1) The full width at half maximum of the elastic peak increases from 6.5 meV on the clean surface up to 16.0 meV for a coverage of 2.5 Å of silver, and then decreases back to its original value as the metal coverage is increased from 3.4 to 17 Å. (2) The structures observed at 12—13 and ~36.2 meV are progressively attenuated as the silver thickness increases. This attenuation is nearly complete at 2.5 Å of silver and is complete within experimental limits at coverages of 3.4 Å and greater. (3) In addition to losses centered at zero frequency, a distinct background wing is seen to develop and increase out to coverages of 2.5 Å. Beyond this coverage the background wing decreases and by the time 17 Å of silver has been deposited the wing intensity is reduced to the noise level.

The following LEED/Auger observations were also recorded at 170 K after the energy-loss spectra were measured. The LEED substrate pattern was observed to wash out for all deposition coverages between 1.7 and 17 Å. This indicates that for a deposition temperature of 170 K, the overlayer is disordered rather than exhibiting nucleated epitaxial registry as has been reported for Ag overlayer growth at room temperature and above.[2,3] We also observed that the ratio of Ga MNN to As MNN peak heights involving the 1070- and 1228-eV transitions remained constant at 1.38 ± 0.02, thus indicating that replacement reactions and segregation have not occurred during the deposition. For the 17-Å coverage neither Ga nor As could be detected. Furthermore, Auger-electron spectroscopy (AES) showed increased attenuation of the substrate low-energy transitions (<100 eV) relative to the high-energy transitions (>1000 eV). Finally, experiments run with substrate temperatures as low as 120 K and silver deposition rates varying between ~0.5 and 2 Å/min gave similar results.

B. Silver island formation

Figures 3 and 4 present EELS data pertinent to the question of whether one obtains uniform overlayer growth or islandlike formation during low-temperature silver deposition on GaAs. The discussion of the next section will show that these spectra can be assigned to scattering

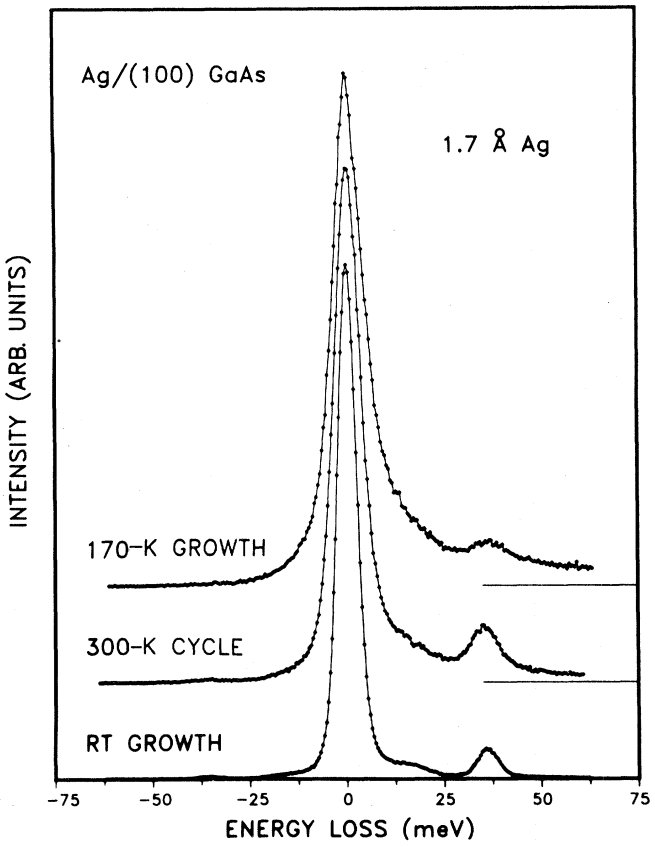

FIG. 4. High-resolution EELS spectra of a 1.7-Å uniform silver overlayer deposited at 170 K (top trace) and after slowly warming to room temperature overnight (middle trace). The spectrum shown in the bottom trace is for a similar sample grown at 300 K.

from silver island films. The data in Fig. 3 pertain to a sample in which 3.4 Å of silver was deposited at ~170 K. After taking the initial energy-loss spectrum (upper trace), the sample was slowly warmed to room temperature overnight, re-cooled to 170 K, and the data in the lower trace recorded. A similar cycle was employed for the 1.7-Å overlayer as well as performing a growth run at room temperature rather than at 170 K. These results are shown in Fig. 4. One notes the following. (1) After a room-temperature cycle, films initially deposited at 170 K show elastic peak narrowing (to ~8 meV FWHM), recovery of most of the $\tilde{\omega}_+$/surface optical phonon intensity at 36.2 meV, clear evidence for the $\tilde{\omega}_-$ mode at 12–13 meV, and significant reduction of the background. In addition, the elastic peak has increased approximately one order of magnitude in intensity. Although the surface is far rougher on a microscopic scale in this instance, the increased intensity is presumably due to the specularity of the scattering from the exposed, well-ordered substrate. (2) Room-temperature growth of very thin layers (~1.7-Å thick) shows stronger features at 36.2 meV and less background than samples with the same overlayer thickness which have undergone low-temperature deposition followed by a room-temperature cycle.

LEED observations of the above samples clearly show substrate diffraction patterns. A high background intensity indicative of surface disorder was also noted. In addition, a few "extra" spots (in no apparent registry with the substrate), presumably due to large, well-ordered silver islands were also observed. Finally, in contrast to the samples discussed in Sec. III A, Auger analysis of these samples show both the high-energy *and* the low-energy GaAs transitions. We see no evidence for either Ga or As segregation, however.

IV. DISCUSSION

In this section we are concerned with reconciling the experimental results presented in Sec. III with theoretical models which treat the electron-energy-loss scattering from a generalized three-layer system (vacuum, metal overlayer, substrate). Two cases will be treated explicitly; the first, that of a uniform metallic overlayer, and the second that of isolated metallic islands. The theoretical expectations for these two cases will be seen to differ substantially.

Our model is one in which each medium is viewed as a dielectric, described by a suitable dielectric constant. Electric field fluctuations in the vacuum above the crystal are responsible for scattering the electron in the dipole scattering models used here. Earlier comparisons between such a theory and experiment show that this picture provides a quantitative description of near-specular electron energy losses, in the range of energies used in the present experiment.[7] In this picture, it is the collective excitations of the conduction electrons in the metal film, along with the surface optical phonon on GaAs that produce the electric field fluctuations responsible for the scattering. One may inquire if particle-hole excitations within the silver film, omitted in our model, also contribute substantially to the loss cross section. Recently, Eguiluz[8] has completed a very detailed theoretical study of the electron-energy-loss cross section for backscattering from a thin jellium film; the particle-hole excitations are included fully in his treatment. They contribute prominently in the limit of large wave-vector transfer (wave-vector change of electron comparable to $2k_F$, with k_F the Fermi wave vector), but at the small momentum transfers of interest here, their contribution is negligible. Thus, our view is that the model we use here contains the essential physics.

A. Uniform metallic overlayer

Since the experiment measures only small angle deviations ($\pm 1°$) from the specular direction, the dipole mechanism will provide the dominant mode for coupling the incoming electron to excitations of the generalized three-layer system.[1] It is therefore appropriate to describe the sample in a macroscopic picture and our model is shown in the insert to Fig. 5. The GaAs substrate is viewed as a dielectric, with frequency-dependent dielectric constant given by

$$\epsilon_B(\omega)=\epsilon_\infty^{(B)}+\frac{(\epsilon_0^{(B)}-\epsilon_\infty^{(B)})\omega_{\mathrm{TO}}^2}{\omega_{\mathrm{TO}}^2-\omega^2-i\omega\Gamma} \quad (1)$$

with ω_{TO} the transverse-optical phonon frequency of the material. This is overlaid by a silver film, here regarded

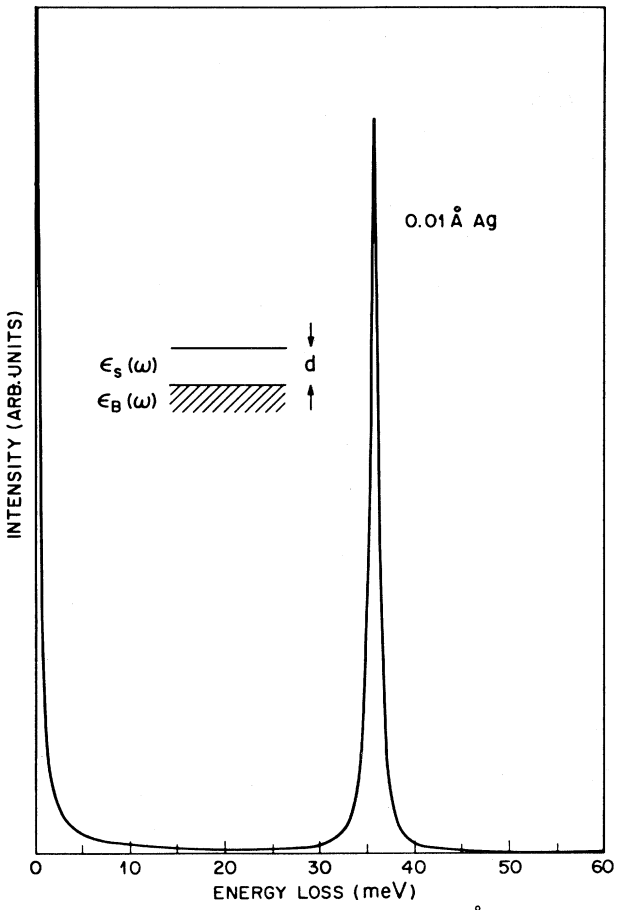

FIG. 5. Calculated EELS spectrum of 0.01-Å-thick uniform overlayer of silver on GaAs. The model employed in the present analysis is shown in the insert. The GaAs substrate is viewed as a semi-infinite dielectric medium with dielectric constant $\epsilon_B(\omega)$ and the Ag film a thin dielectric layer of thickness d, with dielectric constant $\epsilon_s(\omega)$.

as a thin dielectric layer of thickness d described by a dielectric constant

$$\epsilon_s(\omega)=\epsilon_\infty^{(s)}-\frac{\omega_p^2}{\omega(\omega+i\gamma)}\ , \tag{2}$$

where ω_p is the conduction-electron plasma frequency.

An expression for the inelastic electron-scattering cross section in the dipole regime was derived in an earlier work[9] for this geometry. If $d^2S/d\Omega(\hat{k}_s)d\omega$ is the scattering efficiency per unit solid angle $d\Omega(\hat{k}_s)$ per unit frequency $d\omega$, then we may write, once certain assumptions[1,10] reasonable in the present circumstances are invoked,

$$\frac{d^2S}{d\Omega(\hat{k}_s)d\omega}=\frac{2e^2m^2v^4}{\pi\hbar^4\cos\theta_i}\frac{|R_1|^2P(\vec{Q}_{||},\omega)}{[v_\perp^2Q_{||}^2+(\omega-\vec{v}_{||}\cdot\vec{Q}_{||})^2]^2}\ . \tag{3}$$

Here e and m are the electron charge and mass, $\vec{v}_{||}$ and $v_\perp$ the velocity parallel and perpendicular to the surface, θ_I the angle of incidence of the beam (measured from the normal), and $|R_I|^2$ the intensity of the elastic specular beam. The energy loss is $\hbar\omega$, and $\vec{Q}_{||}$ the wave-vector change of the electron, after projection onto a plane parallel to the surface. Kinematical relations may be used to relate $\hbar\omega$ and $\vec{Q}_{||}$ to the angular deflection suffered by the electron.[1,11] Finally $P(\vec{Q}_{||},\omega)$, for the present model, may be written

$$P(\vec{Q}_{||},\omega)=\frac{2\hbar Q_{||}}{\pi}[1+\bar{n}(\omega)]\mathrm{Im}\left[\frac{-1}{1+\bar{\epsilon}(Q_{||},\omega)}\right]\ , \tag{4}$$

where $\bar{n}(\omega)=[\exp(\hbar\omega/k_BT)-1]^{-1}$, and

$$\bar{\epsilon}(Q_{||},\omega)=\epsilon_s(\omega)\left[\frac{1+\Delta(\omega)\exp(-2Q_{||}d)}{1-\Delta(\omega)\exp(-2Q_{||}d)}\right] \tag{5}$$

with

$$\Delta(\omega)=\frac{\epsilon_B(\omega)-\epsilon_s(\omega)}{\epsilon_B(\omega)+\epsilon_s(\omega)}\ . \tag{6}$$

A series of numerical calculations of the energy-loss spectrum have been carried out using the expressions given above. We describe the results of these, then discuss the physical interpretation of these calculations relevant to the data presented in Sec. III.

The experiment does not measure the angular distribution of the inelastically scattered electrons, as described in detail by Eq. (3), but instead collects all electrons which emerge near the specular direction after suffering energy loss. The angular range sampled is controlled by the slit width of the spectrometer. We simulate this by constructing a scattering efficiency per unit frequency interval by integrating Eq. (3) over the range of wave vectors sampled in the experiment. We have

$$\frac{dS}{d\omega}=\int_{|\vec{Q}_{||}|<Q_c}d^2Q_{||}\left[\frac{d\Omega(\hat{k}_s)}{d^2Q_{||}}\right]\frac{d^2S}{d\Omega(\hat{k}_s)d\omega}\ , \tag{7}$$

where a simple expression for $d\Omega(\hat{k}_s)/d^2Q_{||}$ is found elsewhere.[11] In Eq. (7), Q_c is a cutoff wave vector, chosen to mimic the spectrometer slit width ($\sim 1°$ in this case). When the procedure in Eq. (7) is carried out, the angular integration over the direction of $\vec{Q}_{||}$ may be solved analytically. An explicit expression for the result is given elsewhere.[12] Then we numerically compute the integral over the magnitude of $\vec{Q}_{||}$. In the calculations reported below, we have assumed the energy of the incident electrons is 5 eV, and the angle of incidence is 60°. We let $\Gamma=0.03\omega_{TO}$, and for the conduction-electron relaxation rate in the Ag film, we used $\hbar\gamma=0.2$ eV (corresponding to a relaxation time of 0.3×10^{-14} sec for the conduction electrons). The static and high-frequency dielectric constants for GaAs are 12.9 and 10.9, respectively. The remaining parameters are well known for each material.

In Fig. 5 , we show the loss spectrum calculated for the case where the Ag film is very thin, $d=0.01$ Å. While such a small value of d is unphysical, it will be of interest to explore the influence of the screening provided by submonolayer quantities of conducting material distributed uniformly over the surface. The prominent feature near 36 meV is the loss peak from the GaAs surface-optical phonon, here virtually unaffected by the very thin con-

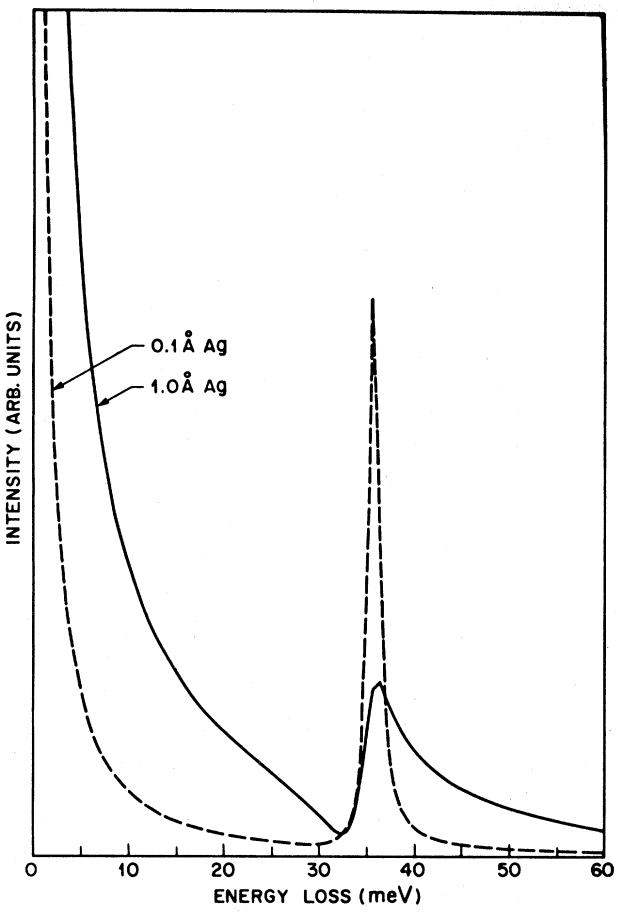

FIG. 6. Theoretical EELS spectra of GaAs covered by a 0.1-Å- (dashed curve) and 1.0-Å- (solid curve) thick uniform overlayer of silver.

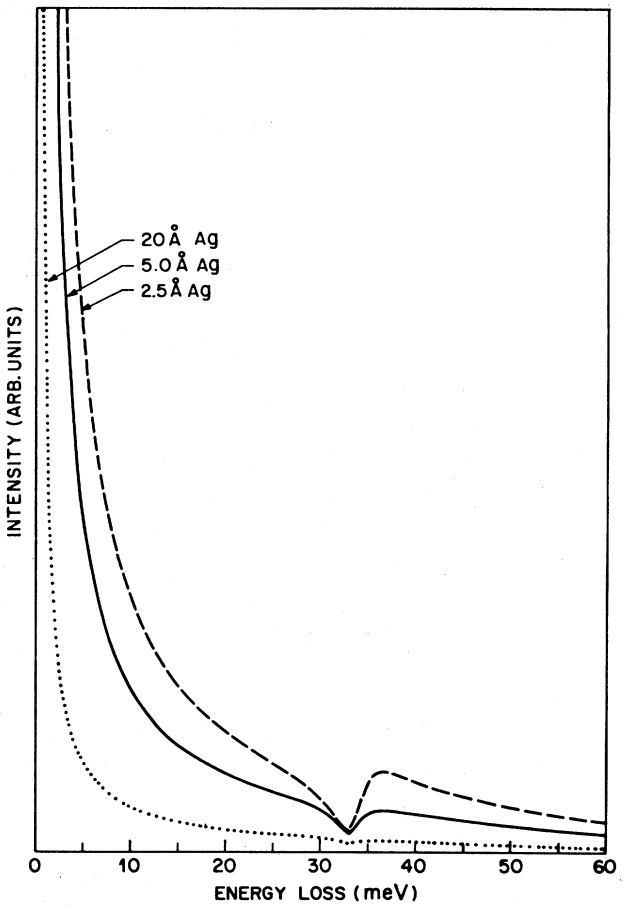

FIG. 7. Theoretical EELS spectra of GaAs covered by a 2.5-Å- (dashed curve), 5-Å- (solid curve) and 20-Å- (dotted curve) thick uniform overlayer of silver.

ducting overlayer. The contribution to the loss spectrum from the electrons in the Ag film appears at very small energy losses, to produce the "central peak" which appears here in the 1—2-meV energy-loss range. In the experimental measurements, the elastic peak will be superimposed on this inelastic contribution. In Fig. 6 we show the loss structure for a GaAs crystal covered by an Ag film 0.1-Å thick (dashed curve). The GaAs surface phonon appears with rather smaller intensity, and the low energy-loss structure is now prominent, even for a conducting layer this thin. By the time the conducting film is only 1-Å thick (Fig. 6, solid curve), the feature from the surface phonon is weaker than that in Fig. 5 by a factor of five, the central peak is now the dominant feature in the spectrum, and the surface phonon feature is distinctly asymmetric. In the dashed curve of Fig. 7, the Ag film thickness is increased to 2.5 Å. The surface mode feature is almost fully suppressed, and it appears as a highly asymmetric dip in the very broad central peak. By the time the Ag film is 5-Å thick (Fig. 7, solid curve), the loss feature appears as a very small dip, and when $d=20$ Å, the dip is barely perceptible (Fig. 7, dotted line).

A number of distinct features relevant to the present experiments emerge from the calculations. One notes immediately the additional inelastic scattering intensity of the central peak whose peak width increases out to a coverage of ~ 2.5 Å and then decreases as the coverage progressively is increased. The high-frequency (~ 60 meV) wing associated with this central peak shows similar behavior. Both of these features are implicit in the experimental data in the observations of the full width at half maximum of the elastic peak and background intensity. Perhaps the most striking feature of the calculations is the rapid attenuation of the substrate surface optical phonon, even for very thin metallic layers. Although this feature is readily detected in the data, due to limited signal-to-noise, we are at present unable to verify the theoretically predicted dip or the conversion of the surface phonon line shape into an asymmetric line.

The features observed above may be understood in relatively simple physical terms if one considers the nature of the surface excitations associated with the uniform overlayer structure.[13] Consider first the interface between GaAs and vacuum, and a thin metal film of thickness d, also surrounded by vacuum. We may imagine the thin film of silver in free space, far from the GaAs substrate. The GaAs surface supports a surface optical phonon, with frequency ω_s determined by the condition $\epsilon_B(\omega_s)=-1$. This gives, from Eq. (1) with $\gamma=0$, $\omega_s=\omega_{\rm TO}([1+\epsilon_0^{(B)}]/[1+\epsilon_\infty^{(B)}])^{1/2}$, where $\epsilon_0^{(B)}$ is the static dielectric

constant of GaAs. The Ag film has two surface modes for each choice of $Q_{||}$. The first of these, in the limit $Q_{||}d \ll 1$ relevant to the present discussion, lies very close to the bulk plasma frequency of Ag, where $\epsilon_s(\omega)=0$. This is beyond the visible range of frequencies, and this mode plays no role in the present analysis. The second, however, is described by a dispersion relation which gives vanishing frequency as $Q_{||}\to 0$. For the isolated film, in the regime $Q_{||}d \ll 1$, for this mode we have $\omega_{Ag}(Q_{||})=\omega_p(Q_{||}d/2)^{1/2}$ with ω_p the plasma frequency which appears in Eq. (2).

When the Ag film is brought close to the GaAs substrate, or overlaid on it, the low-frequency Ag surface mode will interact with the GaAs surface optical phonon, to produce new modes of the structure that are admixtures of these two. The dispersion relations of the new modes are readily found by noting that they appear as poles in the loss function in Eq. (4). In the absence of phonon and plasmon damping ($\gamma=\Gamma=0$), the condition $1+\tilde{\epsilon}(Q_{||},\omega)=0$ gives

$$\frac{[\epsilon_s(\omega)+1]}{[\epsilon_s(\omega)-1]}\frac{[\epsilon_s(\omega)+\epsilon_B(\omega)]}{[\epsilon_s(\omega)-\epsilon_B(\omega)]}=e^{-2Q_{||}d} . \tag{8}$$

We are interested in the regime where $Q_{||}d \ll 1$, and $\omega \ll \omega_p$, so $|\epsilon_s(\omega)| \cong |-\omega_p^2/\omega^2| \gg 1$. Then the left hand side of Eq. (8) is approximated by

$$\frac{\left[1+\frac{1}{\epsilon_s(\omega)}\right]\left[1+\frac{\epsilon_B(\omega)}{\epsilon_s(\omega)}\right]}{\left[1-\frac{1}{\epsilon_s(\omega)}\right]\left[1-\frac{\epsilon_B(\omega)}{\epsilon_s(\omega)}\right]} \cong 1+\frac{2}{\epsilon_s(\omega)}[1+\epsilon_B(\omega)] , \tag{9}$$

while the right-hand side is replaced by $1-2Q_{||}d$. Then with, once again, $\epsilon_s(\omega)=-\omega_p^2/\omega^2$, we are lead to the secular equation

$$\omega^4-\omega^2[\omega_s^2+\omega^2(Q_{||})]+\omega_{TO}^2\omega^2(Q_{||})=0 , \tag{10}$$

where

$$\omega_s^2=\omega_{TO}^2\left[\frac{\epsilon_0^{(B)}+1}{\epsilon_\infty^{(B)}+1}\right] \tag{11a}$$

is the surface optical phonon frequency for a GaAs/vacuum interface, and

$$\omega^2(Q_{||})=\frac{\omega_p^2 Q_{||}d}{(1+\epsilon_\infty^{(B)})} \tag{11b}$$

is the dispersion relation of the low-frequency surface mode of the conduction electrons in a thin metal film with vacuum above, and substrate with frequency-independent dielectric constant $\epsilon_\infty^{(B)}$ below.

From Eq. (10), the dispersion relations of the new coupled modes read

$$\omega_\pm^2(Q_{||})=\tfrac{1}{2}[\omega_s^2+\omega^2(Q_{||})] \pm \tfrac{1}{2}\{[\omega_s^2-\omega^2(Q_{||})]^2 + 4(\omega_s^2-\omega_{TO}^2)\omega^2(Q_{||})\}^{1/2} . \tag{12}$$

An important parameter is the wave vector Q_0 for which

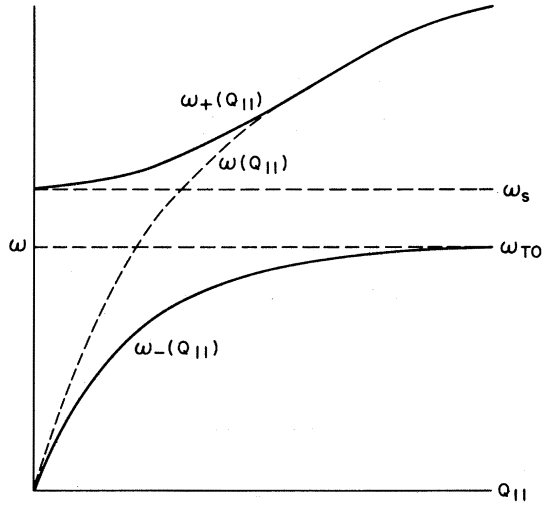

FIG. 8. The collective modes at the surface of GaAs with a thin metal overlayer. The various quantities in the figure are defined in the text.

the low-frequency collective mode of the film crosses the GaAs surface optical phonon frequency. This is determined by setting $\omega_s=\omega(Q_0)$, and we have

$$Q_0=\frac{1}{d}\left[\frac{\omega_{TO}}{\omega_p}\right]^2(1+\epsilon_0^{(B)}) . \tag{13}$$

The dispersion relations in Eq. (12), illustrated in Fig. 8, have the following limiting behavior.

(i) $Q_{||} \ll Q_0$:

$$\omega_+^2(Q_{||}) \cong \omega_s^2+\frac{(\omega_s^2-\omega_{TO}^2)}{\omega_s^2}\omega^2(Q_{||})+\cdots , \tag{14a}$$

so $\omega_+(Q_{||})\to\omega_s$ as $\vec{Q}_{||}\to 0$, and

$$\omega_-^2(Q_{||})=\frac{1+\epsilon_\infty^{(B)}}{1+\epsilon_0^{(B)}}\omega^2(Q_{||}) \equiv \frac{\omega_p^2 Q_{||}d}{1+\epsilon_0^{(B)}} , \tag{14b}$$

the frequency of a surface mode in a thin conducting film placed on a substrate with dielectric constant $\epsilon_0^{(B)}$.

(ii) $Q_{||} \gg Q_0$: Then

$$\omega_+^2(Q_{||}) \simeq \omega^2(Q_{||})-(2\omega_{TO}^2-\omega_s^2)+\cdots , \tag{15a}$$

while

$$\omega_-^2=\omega_{TO}^2+\cdots \tag{15b}$$

approaches the TO phonon frequency of the GaAs film.

Now consider the implications of the above results, from the point of view of electron scattering from the surface. First, note that for GaAs, ω_s and ω_{TO} lie very close to each other, so for the purposes of this discussion, we shall ignore the difference between the two frequencies. The features in the calculated loss spectrum near ω_s or ω_{TO} are produced by scattering off collective excitations on the ω_+ branch, for wave-vector transfers $0 \le Q_{||} \le Q_0$, and from excitations on the ω_- branch for wave-vector transfers larger than Q_0. The crucial issue is then the strength of the electric field fluctuations in the vacuum set up by these two segments of the dispersion curve. As

$Q_{||} \to 0$, the ω_+ branch approaches ω_s which shows that for $Q_{||} \ll Q_0$, the GaAs surface optical phonon is not affected by the presence of the Ag film. It thus produces electric fields with strength unaffected by the overlayer. When $Q_{||} \gg Q_0$, in essence the GaAs surface mode is driven down in frequency to ω_{TO}. But any oscillation of the lattice of an ionic crystal will fail to generate a macroscopic electric field, if the oscillation frequency is ω_{TO}. This is true independent of the spatial variation of the lattice motion.[14]

Thus the crucial issue is whether $Q_c > Q_0$, or $Q_c < Q_0$, where Q_c is the maximum wave vector accepted by the spectrometer. If $Q_c < Q_0$, the feature near ω_s or ω_{TO} is produced by scattering off the ω_+ branch; these modes generate an electric field comparable in strength to that associated with the bare GaAs surface, and we see the surface optical phonon at full strength in the loss spectrum. On the other hand, if $Q_c \gg Q_0$, nearly all electrons collected by the spectrometer have suffered momentum transfers very large compared to Q_0, and in this region of phase space, we have no collective modes near ω_s or ω_{TO} which generate a macroscopic field; the loss peak is absent or very weak. We may define a critical film thickness d_c by setting Q_0 equal to Q_c. Then, if $d \gg d_c$, the GaAs surface optical phonon is suppressed by the Ag film, while if $d < d_c$, it is present with substantial strength. We have, from Eq. (13),

$$d_c = \frac{1}{Q_c} \left[\frac{\omega_{TO}}{\omega_p} \right]^2 (1+\epsilon_0^{(B)}) \ . \tag{16}$$

For parameters characteristic of GaAs with an Ag overlayer ($Q_c \sim 10^6$ cm^{-1}, $\omega_{TO} \sim 33$ meV, $\omega_p \sim 3.5$ eV, and $\epsilon_0^{(B)} \sim 13$), one has $d_c \cong 0.1$ Å, so one monolayer of Ag is quite sufficient to suppress the scattering from GaAs surface optical phonons.

Summarizing this section, we see clearly that as the Ag film thickness increases, a prominent feature centered at zero energy loss appears in the theory, with a wing that falls off slowly with increasing energy loss. This feature has its origin in scattering of the incoming electron off of the low-frequency collective mode of the metal overlayer,[15] described by Eq. (11b) for all frequencies except for those near ω_{TO} or ω_s [for GaAs, $\epsilon_0^{(B)}$ and $\epsilon_0^{(B)}$ differ little from each other, so Eq. (14b) produces a dispersion curve very similar to Eq. (11b)]. In the data, one very clearly sees a wing develop in the loss spectrum as the silver thickness increases, as in the theory. The theory shows that this feature first increases with increasing Ag film thickness, but reaches maximum intensity when $d \cong 2.5$ Å, and then decreases with a further increase in film thickness. Very similar behavior is seen in the data; compare, for example, the spectrum for the GaAs crystal covered by a 3.4-Å Ag film with that covered by a 2.5-Å film. The background is almost totally absent from the data by the time $d = 17$ Å, in accord with theory. Since the background has its origin in scattering off the low-frequency collective mode of the thin film, it follows from its presence in the data that a uniform overlayer has been formed.

B. Metallic island growth

The fact that one monolayer of Ag serves to suppress the GaAs surface phonon depends crucially on the assumption that the Ag is present as a smooth film that supports a long wavelength, low-frequency collective mode which couples to the GaAs surface mode over a wide range of phase space, thus suppressing its macroscopic field. If a monolayer's worth of Ag is instead collected into islands that are each roughly hemispherical, with ΔR a measure of the linear dimensions of a typical patch of open GaAs surface, the hemispheres will be unable to screen those GaAs modes with $Q_{||} \Delta R > 1$, since such short-wavelength modes may propagate on those portions of the GaAs surface unaffected by the silver. Thus, if $\Delta R \gtrsim Q_c^{-1}$, the surface optical phonon signal will be strong. In addition, hemispherical Ag islands only have collective modes in the visible frequency range, near the plasma frequency $\omega_p/(2+\epsilon_\infty^{(s)})^{1/2}$ of a Ag film.[16] The absence of a low-frequency collective mode for the Ag islands means that neither a central peak nor a substantial high-frequency (60 meV) wing are anticipated.

These predictions are born out in detail in Figs. 3 and 4, particularly for the case where 1.7 Å of Ag was deposited onto a room-temperature substrate. The surface optical phonon is not quenched to any measurable extent nor does one observe the significant background and broadening of the elastic peak seen in the data of Figs. 1 and 2. For situations where the film was deposited at 170 K and then cycled to room temperature, one sees something akin to intermediate behavior, i.e., an increase in the surface optical phonon and decrease, but not extinction of the background. We interpret this observation to mean that island formation under these conditions is not complete and that sections of the sample surface remain with patches of uniform overlayers coexisting with Ag islands and undecorated substrate areas. The conversion appears to be coverage dependent, since the data for a 3.4-Å film cycled to room temperature show more "islandlike" features than the 1.7-Å data similarly cycled.

Analysis of Figs. 1 and 2 in terms of the growth of a uniform silver film and Figs. 3 and 4 in terms of metal island formation is consistent with our LEED and Auger measurements. Low substrate temperatures during metal deposition produced no LEED patterns, while cycling the sample to room temperature always resulted in the observation of diffraction patterns characteristic of the substrate. For pinholes in an overlayer on the order of hundreds of angstroms, one would expect to observe substrate LEED patterns. Furthermore, previous studies of Ag/(100) GaAs at room temperature show evidence for nucleated growth.[3] Analysis of our Auger data corroborates these findings: low-temperature silver depositions show increased attenuation of the low-energy Ga and As transitions due to the shorter escape depth of these electrons. Finally lowering the substrate temperature to 170 K during the metal evaporation should minimize surface diffusion. This temperature is certainly low enough to quench island formation since spectra recorded for silver depositions on substrates cooled to 120 K are very similar.

V. SUMMARY

In this paper we have shown that thin, conducting overlayers deposited onto ionic crystal surfaces can completely quench inelastic electron scattering from substrate vibrational modes. Low-frequency collective modes characteristic of *uniform* film growth have also been observed. These new features are not found when the deposited atoms coalesce into small islands. Thus EELS may provide a new and potentially important method for studying the structure of thin metal films.

ACKNOWLEDGMENTS

The research of R.E.C. and D.L.M. has been supported by the U.S. Department of Energy, through Contract No. DEAT-0379-ER-10432. We thank D. L. Allara for the loan of equipment during the course of these experiments and D. R. Falcone for help in calibrating the quartz crystal oscillator.

---

[1]See H. Ibach and D. L. Mills, *Electron Energy Loss Spectroscopy and Surface Vibrations* (Academic, New York, 1982), and references cited therein.

[2]J. Massies and N. T. Linh, J. Cryst. Growth 56, 25 (1982).

[3]R. Ludeke, T.-C. Chiang, and D. E. Eastman, J. Vac. Sci. Technol. 21, 599 (1982).

[4]B. A. Sexton, J. Vac. Sci. Technol. 16, 1033 (1979).

[5]R. Matz and H. Lüth, Phys. Rev. Lett. 46, 500 (1981).

[6]L. H. Dubois and G. P. Schwartz, J. Vac. Sci. Technol. B (to be published).

[7]A number of examples are given in Chap. 3 of Ref. 1.

[8]A. Eguiluz, Phys. Rev. Lett. 51, 1907 (1983).

[9]H. Froitzheim, H. Ibach, and D. L. Mills, Phys. Rev. B 11, 4980 (1975).

[10]D. L. Mills, Surf. Sci. 48, 59 (1975).

[11]E. Evans and D. L. Mills, Phys. Rev. B 5, 4126 (1972).

[12]R. E. Camley and D. L. Mills, Phys. Rev. B (to be published).

[13]In these experiments the wave vector $\vec{Q}_{||}$ of the modes excited by the incident electron beam is very large (typically 10^6 cm^{-1}) compared to ω/c, with c the velocity of light, so the influence of retardation may be ignored.

[14]To see this, just note that if $\vec{u}(\vec{x})$ is the amplitude of the vibration of the lattice (the relative displacement of the atoms in the unit cell, appropriate to optical phonons of long wavelength), then the macroscopic field $\vec{E}(\vec{x})$ generated by the lattice motion is given by $e_T^*\vec{E}(\vec{x})=M_r(\omega_{TO}^2-\omega^2)^2\vec{u}(\vec{x})$, where e_T^* is the transverse effective charge, and M_r the reduced mass of the unit cell. If $\omega=\omega_{TO}$, then $\vec{E}(\vec{x})\equiv 0$, independent of the spatial form of $\vec{u}(\vec{x})$.

[15]Although one might argue that surface roughness will cause the elastic peak to broaden significantly, this cannot explain the uniform background intensity since it is not symmetric about the zero-energy loss peak.

[16]See, for example, P. C. Das and J. I. Gersten, Phys. Rev. B 25, 6281 (1982).